prior bilateral Descemet's stripping automated endothelial keratoplasty (DSAEK), with repeat DSAEK to left eye, bilateral cataract surgery with posterior intraocular lens (PCIOL) placement, and trabeculectomy with tube shunt in the left eye. Medications included acetazolamide, brimonidine/timolol ophthalmic solution, bimatoprost ophthalmic solution, topiramate, esomeprazole, clopidogrel, and multivitamins.

On physical examination, the patient had a visual acuity of 20/30 on the right and subjectively no light perception on the left. Both pupils were slightly irregular and postsurgical, 5 mm in size in each eye. The right pupil was reactive to light with a relative afferent pupillary defect present OS. The left pupil did show some reactivity minimally to maximum light stimulation from the indirect ophthalmoscope with controlling of accommodation and fixing with the fellow eye on a distance target with the pupil noted to be unchanged in the unaffected contralateral eye. Both eyes showed full motility. Automated visual field in the remaining right eye demonstrated a superior and inferior glaucomatous arcuate defect. Slit-lamp examination showed prior corneal surgery and the presence of a glaucoma shunt tube OS. There was no evidence of uveitis in the anterior segment and bilateral posterior chamber intraocular lenses.

Ophthalmoscopy showed a normal macula and vessels without findings of vasculitis or vitreous cells OS. Both optic nerves had a markedly cupped nerve to the rim (0.95) OU, but there was also superimposed severe diffuse optic atrophy with rim pallor OS. Optical coherence tomography (OCT) showed markedly reduced global retinal nerve fibre layer values of 28 microns on the left (Fig. 1).

This patient had no light perception vision and marked retinal nerve fibre layer loss (28 microns) OS. There was however, a minimal retained pupillary light reflex. This was present even with the fellow eye covered and also with accommodation controlled. We hypothesize that some patients with no light perception vision may still retain their pupillary light reflex because of the presence of mRGCs. Selective ablation of mRGCs has also been shown to completely negate this pupillary response, further supporting the idea that despite no light perception vision that there might be a retained pupil response.[6] Typically, patients with claimed no light perception vision in one eye have retained pupillary responses. There might be other circumstances however similar to our patient with organic no light perception vision and a partially retained pupil reaction where the patient might mistakenly be assumed to be nonorganic overlay.

Funding: This work was supported in part by an unrestricted grant from Research to Prevent Blindness (RPB) to the University of Texas Medical Branch, Galveston, Texas, USA.

Yang Zhou, [*] **Alexander S. Davis,** [†,‡] **Arielle Spitze,** [‡] **Andrew G. Lee** [*,†,‡,§,¶]

[*]Baylor College of Medicine, Houston; [†]The University of Texas Medical Branch, Galveston; [‡]The Methodist Hospital, Houston, Tex.; [§]Weill Cornell Medical College, New York, N.Y.; and [¶]The University of Iowa Hospitals and Clinic, Iowa City, Iowa

Correspondence to:
Andrew G. Lee, MD: AGLee@tmhs.org

References

1. Li RS, Chen BY, Tay DK, Chan HH, Pu ML, So KF. Melanopsin-expressing retinal ganglion cells are more injury-resistant in a chronic ocular hypertension model. *Invest Ophthalmol Vis Sci*. 2006; 47:2951-8.
2. Feigl B, Mattes D, Thomas R, Zele AJ. Intrinsically photosensitive (melanopsin) retinal ganglion cell function in glaucoma. *Invest Ophthalmol Vis Sci*. 2011;52:4362-7.
3. Kawasaki A, Herbst K, Sander B, Milea D. Selective wavelength pupillometry in Leber hereditary optic neuropathy. *Clin Experiment Ophthalmol*. 2010;38:322-4.
4. Jakobs TC, Libby RT, Ben Y, John SW, Masland RH. Retinal ganglion cell degeneration is topological but not cell type specific in DBA/2J mice. *J Cell Biol*. 2005;171:313-25.
5. La Morgia C, Ross-Cisneros FN, Hannibal J, Montagna P, Sadun AA, Carelli V. Melanopsin-expressing retinal ganglion cells: implications for human diseases. *Vision Res*. 2011;51:296-302.
6. Guler AD, Ecker JL, Lall GS, Haq S, Altimus CM, Liao HW, Barnard AR, Cahill H, Badea TC, Zhao H, Hankins MW, Berson DM, Lucas RJ, Yau KW, Hattar S. Melanopsin cells are the principal conduits for rod-cone input to non-image-forming vision. *Nature*. 2008;453:102-5.

Can J Ophthalmol 2014;49:e20–e21

http://dx.doi.org/10.1016/j.jcjo.2013.10.008

Diffusion-weighted imaging in posterior ischemic optic neuropathy

Diffusion-weighted imaging (DWI) is a magnetic resonance imaging (MRI) sequence that provides image contrast dependent on the molecular motion of water. Acute ischemia in the central nervous system (CNS) results in disruption of normal cellular metabolism with depletion of ATP causing failure of Na^+/K^+ ATPase ionic pumps with loss of ionic gradients across cellular membranes. This causes cytotoxic edema with a net shift of water from the extracellular to the intracellular space and changes in the relative volume of these compartments, as well as alterations in their microenvironments. These rapid biophysical changes result in locally restricted diffusion of water molecules that is readily detected by DWI within minutes of acute onset of ischemia.[1] DWI is highly sensitive (81%–100%) and specific (86%–100%) for detecting acute

ischemic stroke.[1,2] The optic nerve is considered as a direct extension of the CNS, and the pathophysiology of acute intraorbital and intracranial optic nerve ischemia is similar to that seen in the brain. DWI might also be useful for the evaluation of ischemic lesions of the optic nerve especially in posterior ischemic optic neuropathy (PION).[3–6] In contrast with PION, anterior ION (AION) affects primarily the optic nerve head anterior to the lamina cribrosa, and DWI in a few cases with imaging has not proved to be as useful.[7] We present a case of restricted diffusion on DWI in the setting of PION.

To our knowledge, this is the first reported case in English-language literature demonstrating DWI restriction in PION in the setting of presumed alcohol-related seizure disorder and secondary rhabdomyolysis-related renal failure.

A 41-year-old male presented with acute, painless loss of vision in the left eye (OS) after he was found unconscious and unresponsive for at least18 hours. He was admitted to the hospital and discovered to be in acute renal failure caused by rhabdomyolysis. The blood pressure on admission was 154/92 mm Hg. Creatinine phosphokinase (CPK) of 22.188 (35-200) IU/L, blood urea nitrogen was 39 (8–24) mg/dL, creatinine was 3.8 (0.5–1.5) mg/dL, and glomerular filtration rate was 18. Upon awakening, he reported painless vision loss OS. Medical history was significant for hypertension, chronic alcohol abuse, multiple head traumas, and variably controlled presumed alcohol-related seizures. His social history was positive for alcohol abuse of 6 to 18 drinks/day and more over the weekends. Family history was noncontributory. His home medication was lisinopril. He denied any drug allergy.

Visual acuity was 20/25 OD and counting fingers at 2 feet OS. The pupils were isocoric and there was a left relative afferent pupillary defect (RAPD). Confrontation visual field was full OD and showed a central scotoma OS. Motility and intraocular pressure examinations were normal OU. Slit-lamp biomicroscopy was normal OU. Dilated funduscopic examination showed normal fundi OU with cup-to-disc ratios of 0.3 OU.

MRI of the brain and orbits was performed on a 3-Tesla MRI scanner (Signa Excite HDxt; GE Healthcare, Waukesha, Wis.) using an 8-channel head coil. The MRI protocol included coronal DWI, and coronal and axial diffusion tensor imaging (DTI) of the orbits. Orbital DWI and DTI were acquired using SE EPI, TR 14 000 milliseconds, TE 60 to 100 milliseconds, FOV 16 cm,

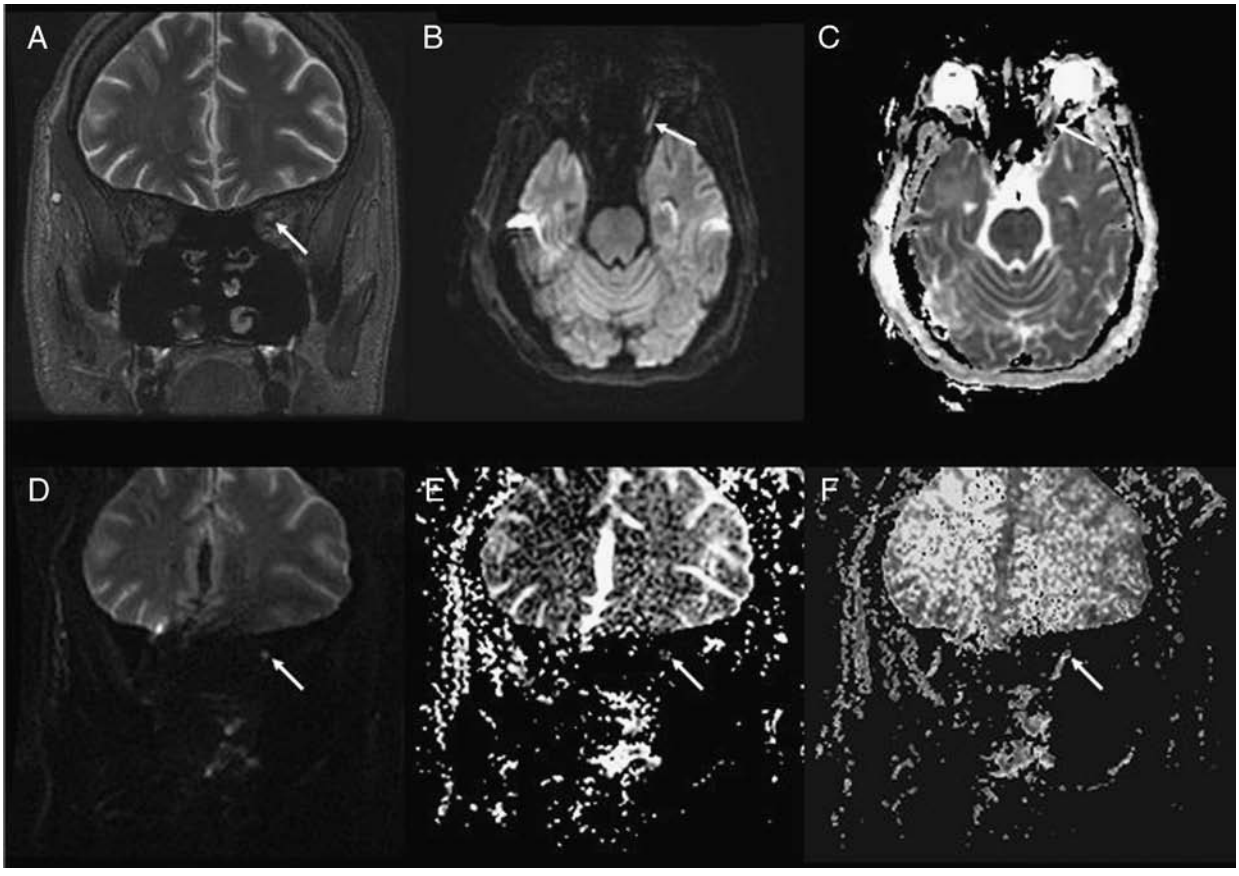

Fig. 1—Magnetic resonance imaging without contrast of orbits: (A) coronal T2-weighted image, (B) axial diffusion-weighted imaging, and (C) apparent diffusion coefficient map show T2 prolongation and restricted diffusion along the orbital segment of the left optic nerve (*arrows*). This is confirmed on (D) coronal diffusion tensor imaging, (E) mean diffusion map, and (F) fractional anisotropy map with restricted diffusion and decreased fractional anisotropy consistent with acute-subacute ischemia along the orbital segment of the left optic nerve (*arrows*).

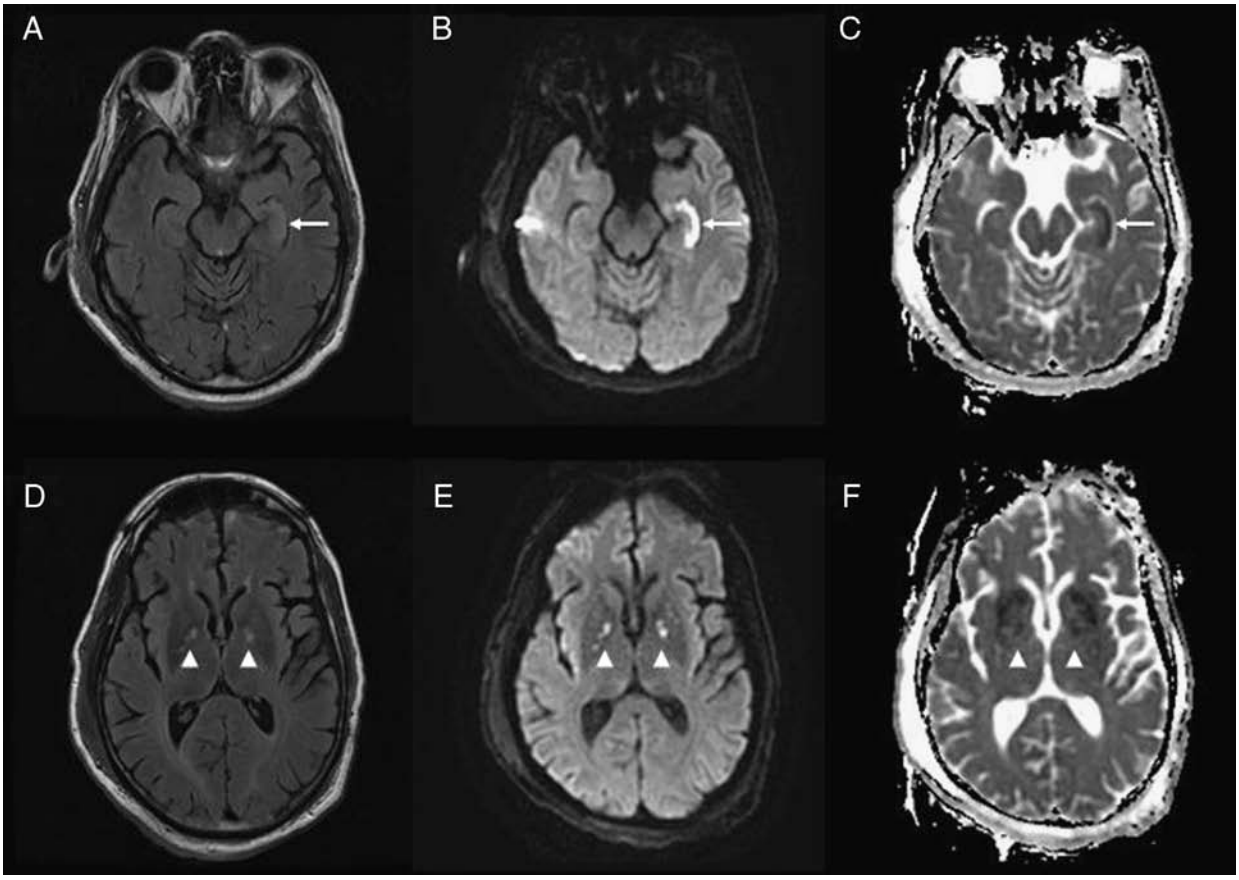

Fig. 2—Magnetic resonance imaging without contrast of the brain. Axial T2 fluid-attenuation inversion recovery (FLAIR) (A, D), diffusion-weighted imaging (B, E), and apparent diffusion coefficient maps (C, F) at the level midbrain (A–C) and basal ganglia (D–F) show T2 prolongation and restricted diffusion within the left hippocampus (*arrows*) and multiple punctuate areas within bilateral globi pallidi and putamina (*arrowheads*), likely because of acute-subacute ischemia given the history of presumed prolonged hypoxic-ischemic episode.

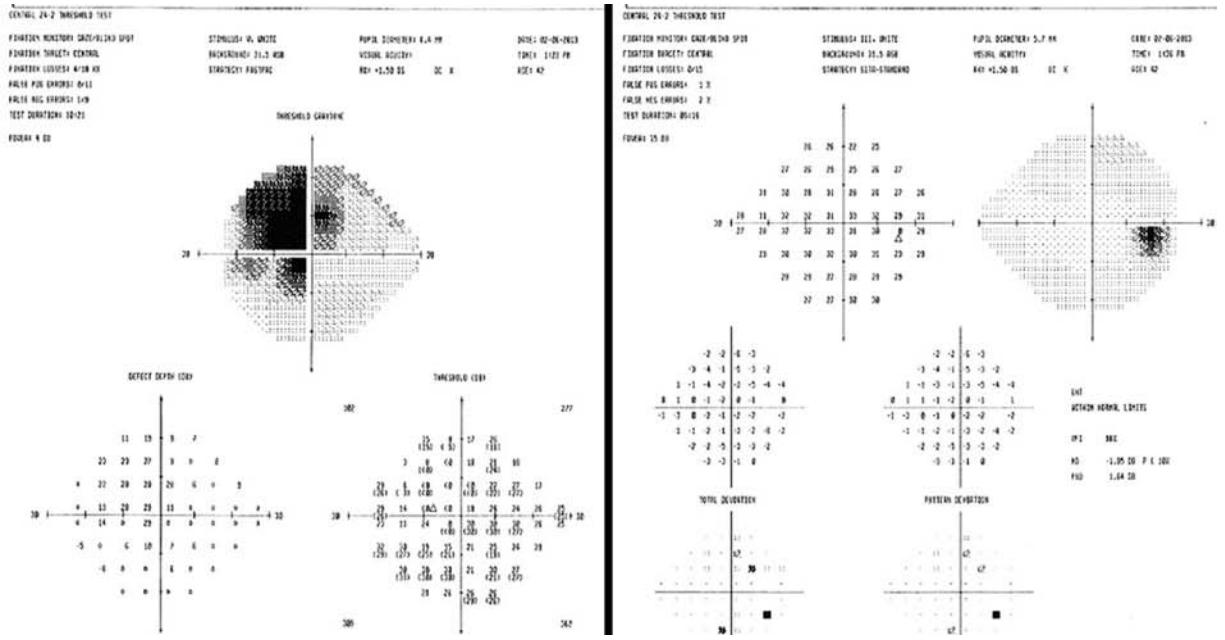

Fig. 3—Humphrey visual field (24-2) 6 weeks after discharge showed central scotoma with breakout superior temporal periphery OS and a normal examination OD.

acquisition matrix 128 × 128, slice thickness 3 mm, and reconstructed to 0.625 mm in-plane resolution. Diffusion-sensitized gradients were applied along 15 noncollinear directions for both coronal and axial DTI. A smaller b value of 200 sec/mm^2 was used for coronal DWI and coronal DTI to reduce distortion from susceptibility artifact, whereas axial DTI was acquired using standard b value of 1000 sec/mm^2. The images showed evidence of cytotoxic edema with reduced diffusion and T2 prolongation along the orbital segment of the left optic nerve, left hippocampus, and bilateral globi pallidi, likely from acute-subacute ischemia given the history of prolonged hypoxic-

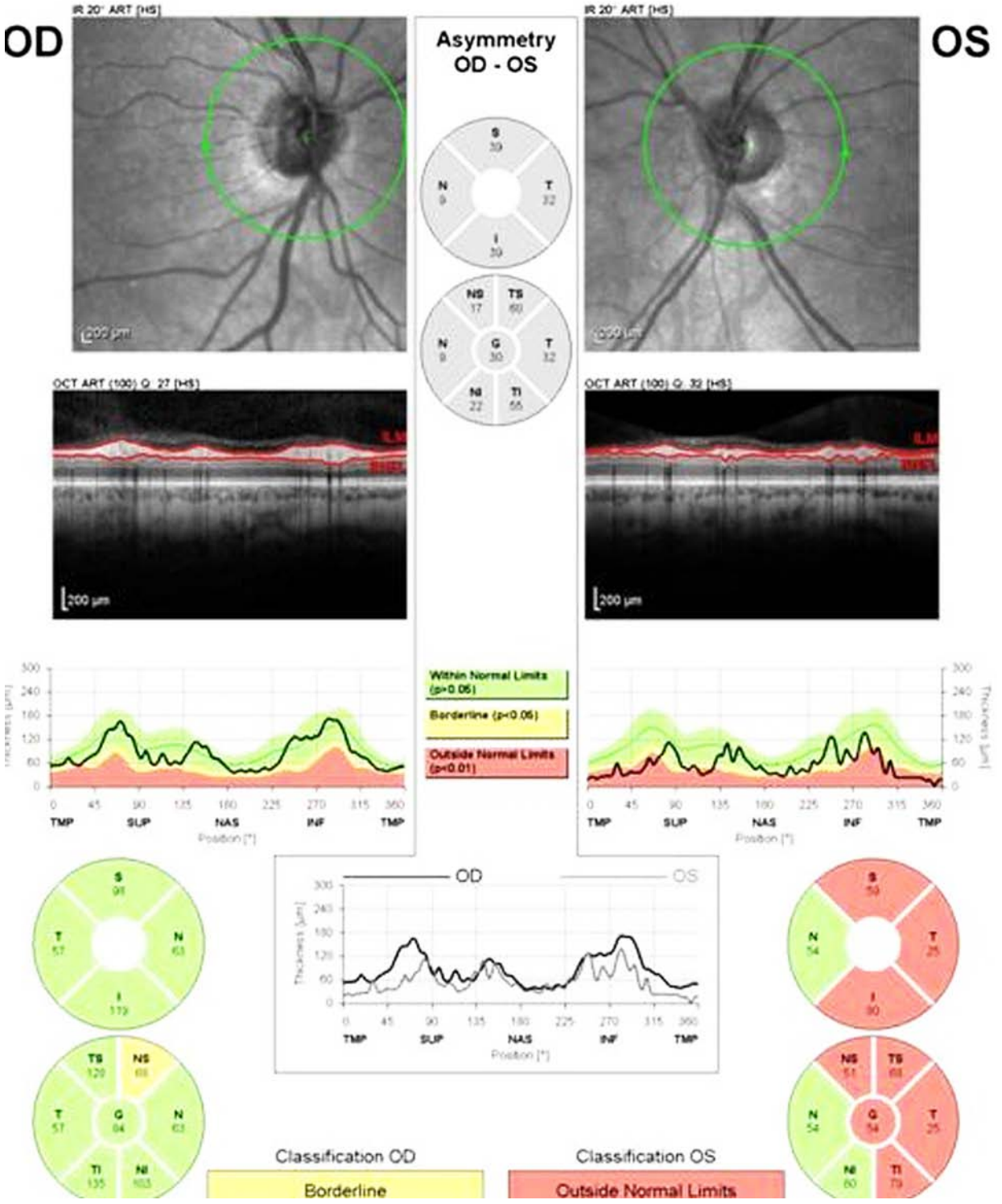

Fig. 4—Optical coherence topography (OCT) of the optic nerves 6 weeks after discharge shows retinal nerve fibre layer loss left eye (OS) and normal right eye (OD). SE, Spin-Echo; EPI, echo planar imaging; TR, repetition time; TE, echo time; FOV, field of view.

ischemic episode (Figs. 1, 2). On a follow-up visit 6 weeks after discharge, there was no change in visual acuity or RAPD OS. Funduscopic examination demonstrated diffuse pallor of the optic nerve OS. Humphrey visual field (24-2) showed a central scotoma with breakout superior temporal periphery visual field defect OS and normal OS (Fig. 3). Optical coherence topography showed reduced retinal nerve fibre layer OS and normal OD (Fig. 4). EEG was normal with no lateralized, epileptiform activity or electrographic seizure recorded.

Ischemic changes along the optic nerve are difficult to detect by DWI, with high likelihood of false-negative results. Susceptibility artifact from adjacent structures and partial volume averaging effect from routine axial DWI acquisition are likely contributing factors. Obtaining images in the coronal plane, acquiring at higher spatial resolution, and increasing signal-to-noise ratio with DTI can improve infarct detection. In this patient, we used a combination of coronal DWI and DTI to image changes from presumed PION. In contrast with PION, AION is due to ischemia at the disc head and produces optic disc edema. AION can be of the arteritic (giant cell arteritis) or nonarteritic form (NAION). In contrast, PION is due to retrobulbar ischemia and no edema is seen in the acute phase. The blood supply to the posterior optic nerve is derived from the pial branches of the ophthalmic artery and may be more susceptible to more global ischemia.[8]

The incidence of AION of both arteritic AION and NAION subtypes combined is 2.66 to 10.66/100,000, whereas the precise incidence of PION is unknown but likely is much lower.[9] The prognosis of perioperative or arteritic PION is poor, whereas the prognosis of nonarteritic, nonsurgical PION is typically better and more closely mirrors the course of NAION.[10] Several case reports have demonstrated the use of DWI for diagnosing an acute optic nerve infarction or acute ION after infection, surgery, or inflammatory or noninflammatory optic neuropathies.[11–15]

In our case, we describe PION with restricted diffusion on the DWI MRI. Although there are 7 prior reported cases of the use of DWI in PION,[3,5–10] to our knowledge, this is the first case report in the English-language literature demonstrating DWI restriction in PION in the setting of presumed alcohol-related seizure disorder and secondary rhabdomyolysis-related renal failure.

Supported by: This work was supported in part by an unrestricted grant from Research to Prevent Blindness.

Nagham Al-Zubidi, [*,†] **Scott Stevens,** [‡] **Steve H. Fung,** [*,†] **Andrew G. Lee** [*,†,‡,§,¶,‖]

[*]Houston Methodist Hospital;[†]Weill Cornell Medical College;[‡]University of Texas Medical School at Houston, Houston, Texas; [§]University of Iowa Hospitals and Clinics, Iowa City, Iowa; [¶]University of Texas Medical Branch, Galveston; and [‖]University of Texas M.D. Anderson Cancer Center, Houston, Texas.

Correspondence to:
Andrew G. Lee, MD: AGLee@HoustonMethodist.org

References

1. Fung SH, Roccatagliata L, Gonzalez RG, Schaefer PW. MR diffusion imaging in ischemic stroke. *Neuroimaging Clin N Am*. 2011;21:345-77.
2. Gonzalez RG, Schaefer PW, Buonanno FS, et al. Diffusion-weighted MR imaging: diagnostic accuracy in patients imaged within 6 hours of stroke symptom onset. *Radiology*. 1999;210:155-62.
3. Purvin V, Kuzma B. Intraorbital optic nerve signal hyperintensity on magnetic resonance imaging sequences in perioperative hypotensive ischemic optic neuropathy. *J Neuroophthalmol*. 2005;25:202-4.
4. Cauquil C, Souillard-Scemama R, Labetoulle M, Adams D, Ducreux D, Denier C. Diffusion MRI and tensor tractography in ischemic optic neuropathy. *Acta Neurol Belg*. 2012;112:209-11.
5. Al-Shafai LS, Mikulis DJ. Diffusion MR imaging in a case of acute ischemic optic neuropathy. *Am J Neuroradiol*. 2006;27:255-7.
6. Klein JP, Cohen AB, Kimberly WT, et al. Diffusion-weighted magnetic resonance imaging of bilateral simultaneous optic nerve infarctions. *Arch Neurol*. 2009;66:132-3.
7. Arnold AC, Hepler RS, Hamilton DR, Lufkin RB. Magnetic resonance imaging of the brain in nonarteritic ischemic optic neuropathy. *J Neuroophthalmol*. 1995;15:158-60.
8. Srinivasan S, Moorthy S, Sreekumar KP, Kulkarni Chinmay. Diffusion-weighted MRI in acute posterior ischemic optic neuropathy. *Indian J Radiol Imaging*. 2012;22:106-7.
9. Khan AA, Hussain SA, Khan M, Corbett JJ. MRI findings of bilateral posterior ischemic optic neuropathy in postcardiac transplant patient. *The Neurologist*. 2012;18:313-5.
10. Park JY, Lee IH, Song CJ, Hwang HY. Diffusion MR imaging of postoperative bilateral acute ischemic optic neuropathy. *Korean J Radiol*. 2012;13:237-9.
11. Wang MY, Qi PH, Shi DP. Diffusion tensor imaging of the optic nerve in subacute anterior ischemic optic neuropathy at 3T. *AJNR Am J Neuroradiol*. 2011;32:1188-94.
12. Le Bihan D, Mangin JF, Poupon C, et al. Diffusion tensor imaging: concepts and applications. *J Magn Reson Imaging*. 2001;13:534-46.
13. Mori S, Zhang J. Principles of diffusion tensor imaging and its applications to basic neuroscience research. *Neuron*. 2006;51:527-39.
14. Lee YJ, Kim HJ, Choi KD, Choi HY. MRI restricted diffusion in optic nerve infarction after autologous fat transplantation. *J Neuroophthalmol*. 2010;30:216-8.
15. Spierer O, Ben Sira L, Leibovitch I, Kesler A. MRI demonstrates restricted diffusion in distal optic nerve in atypical optic neuritis. *J Neuroophthalmol*. 2010;30:31-3.

Can J Ophthalmol 2014;49:e21–e25

http://dx.doi.org/10.1016/j.jcjo.2013.11.003